

Investigation of Inlet Air Fogging as a Heat Transfer Enhancement Technique for Gas Turbines



Hisham Saeed Hashim^{1*}, Muna Sabah Kassim¹, Raid Abd Alwan²

¹ Department of Mechanical Engineering, Engineering College, Mustansiriyah University, Baghdad, Iraq

² Training and Power Researches Office Power Researches Department Ministry of Electricity, Baghdad, Iraq

Corresponding Author Email: ehph003@uomustansiriyah.edu.iq

Copyright: ©2023 IIETA. This article is published by IIETA and is licensed under the CC BY 4.0 license (<http://creativecommons.org/licenses/by/4.0/>).

<https://doi.org/10.18280/ijht.410607>

ABSTRACT

Received: 5 May 2023

Revised: 24 August 2023

Accepted: 5 September 2023

Available online: 31 December 2023

Keywords:

gas turbine, fogging technique, heat transfer enhancement, cost benefit, computational fluid dynamics (CFD)

The ambient temperature's impact on the power output of gas turbines is significantly pronounced, particularly in hot and dry climates such as Iraq. This study seeks to elucidate the potential enhancement of heat transfer and performance improvement in gas turbines through the implementation of an inlet air fogging system. By cooling and humidifying the inlet air, it is hypothesized that the air's density and mass flow rate will be augmented, thereby increasing the power output and overall cycle efficiency. A comprehensive experimental and numerical investigation was undertaken, employing the inlet fogging technique which introduces a mist of fine water droplets into the incoming airflow. The heat exchange between the water droplet surface and the hot air-up until the droplet's evaporation - was examined meticulously. The results underscored differential improvements when using 9 and 5 nozzles, which modified the air velocity flow. These improvements were attributed to the enhancement in heat exchange between the hot air and the evaporating water droplets, leading to an increase in electrical energy output. Computational fluid dynamics (CFD) was employed to analyze the thermal behavior inside the wind tunnel using the commercial software Fluent 22 R1. The model predictions and experimental observations along the duct exhibited satisfactory agreement, with the most significant discrepancies being a temperature drop of 2.5% and a heat transfer rate difference of 3.8%.

1. INTRODUCTION

This study presents an analysis of the CO₂ emissions and energy costs associated with the installation of a high-pressure fogging air intake-cooling system at the Ihovbor gas turbine power plant in Benin City, southern Nigeria. It was found that the application of high-pressure fogging inlet air cooling technology could potentially reduce the emission of CO₂ and other greenhouse gases from power plants [1]. The integration of a fogging air intake cooling system could enhance the economic and environmental advantages of gas turbines. Various cooling methods primarily serve to boost electrical power generation during peak load times. The output power of a combined cycle power plant (CCPP) is directly influenced by the mass flow rate of air through the air compressor. Consequently, during periods of high ambient temperatures, a decrease in air density induces a sharp decline in power output. It was observed that the air temperature within the fogging system could reach wet-bulb temperatures and achieve 100% efficiency. However, the presence of dripping water could potentially damage the compressor [2]. An examination of performance data from the Omotosho Phase II gas turbine power plant in Ondo State, Nigeria, was conducted to identify the output performance requirements of the gas turbine power plant. It was concluded that the integration of fogging systems

could reduce specific fuel consumption and thus achieve cost-effective operation. Furthermore, it was observed that the incorporation of fogging systems in the power plant could minimize greenhouse gas emissions, thereby reducing environmental pollution [3]. A numerical analysis was performed to investigate the impact of reducing the compressor intake air temperature using evaporative cooling fogging. The study examined the effects of various factors, such as air inlet temperature and relative humidity, air and water mass flow rates, water droplet injection speed, and droplet sizes. It was found that the air-to-water thermal condition and the size of the water droplets did not significantly affect the processes of evaporative cooling. Cooling the input air temperature could potentially improve the turbine output power by approximately 1 to 8.1% [4]. The thermal efficiency of gas turbines is a focus of ongoing improvements in their manufacturing process. One of the methods being explored is increasing the turbine input temperature. However, this approach presents several challenges, such as the generation of thermal stresses due to rapid spatial temperature variations within the blade, which can be hazardous. Cooling of the blades is necessary to address issues with thermal loads, creep, and oxidation that limit the life span of turbines. To increase the averages of heat transport, ribs are strategically placed at predictable intervals. However,

the improved heat transfer is accompanied by an increase in pressure drop, which can sometimes be several times larger than that for smooth passage [5]. Previous research has demonstrated the effectiveness of deep cooling to increase ambient air cooling at gas turbine inlet temperatures in temperate climates. A method of logical examination of the actual operation effectiveness of turbine intake air cooling systems in real, variable environments was utilized, reinforced with a basic numerical simulation. According to these findings, cooling turbine intake air to 7 to 10°C in temperate climates using combined absorption-ejector chillers results in an annual fuel savings that is about 50% greater than what is gained from cooling air to 15°C traditionally using an absorption lithium-bromide chiller on a simple cycle [6].

A CFD study demonstrates the enhancement of exhaust gas recirculation's cooling efficiency [7]. Inside the engine compartment of a car, the best of twelve different wing-type vortex generator forms were developed. The percentage area encompasses 10%-28% of the duct's surface area. Carbon dioxide nitride exhaust gas with a temperature of 673 K flows through the inner conduit, while water with a temperature of 353 K flows through the upper and lower channels in the opposite direction. Yu et al. [8] investigated heat transmission in models with two chambers using pin fins and water droplets. In order to simulate the impact of periodic disturbances on circular pin fins and their impact on the heat transfer coefficient, ICEM and CFD were added to the HEXA mathematical models. Experimental analysis by using different types of ribs in the test section on the performance of heat transfer Shapes and cross sections are crucial because they disrupt the boundary layer and induce turbulent flow, which improves heat transmission [9]. Gulave et al. [10] studied the effects of installing rib turbulators in a rectangular duct to improve heat transfer performance. Ribs come in a variety of varieties. Ribs that are circular, M-shaped, W-shaped, and V-shaped. The placement of the ribs is crucial for improving heat transfer. For this experiment, a gas turbine modeled after the General Electric LM6000 engine was used [11]. The turbine generates power to operate both the air compressor of the power plant and the refrigeration cycle compressor of the chiller, according to the mathematical analysis used to evaluate the performance of each component of the gas turbine.

The majority of previous research has predominantly focused on gas power plants in real-world settings. However, in the present study, a laboratory apparatus has been designed to investigate the results according to several variables, most notably the number of nozzles and variable velocity.

The objective of this study is to investigate the performance enhancement and economic benefits of installing an inlet air fogging system for gas turbines.

2. SYSTEM DESCRIPTION

2.1 Bell mouth

The air enters the wind tunnel through a bell-shaped duct that has a 148 cm side square intake and, gradually, becomes a 50 cm side square throughout the 147 cm length section. Figure 1 shows the bell mouth outer surface insulated by using thick (1 mm) rubber foam insulation material of 0.04 W/mK thermal conductivity to prevent any heat interaction with the surrounding environment during the cooling process; Figure 1

shows the schematic. At the beginning of the bell mouthpart, a metallic mesh with 0.01 m square cells is placed to reduce the lateral velocity components brought on by the swirling motion in the airflow during entry. The bell mouth aims to isolate any entrance effects and produce steadily flowing air, as illustrated in Figure 2.

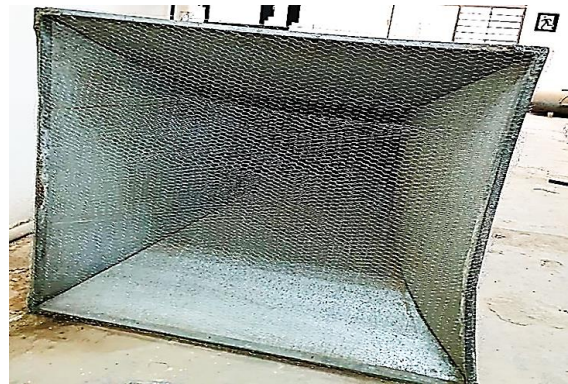


Figure 1. Bell mouth

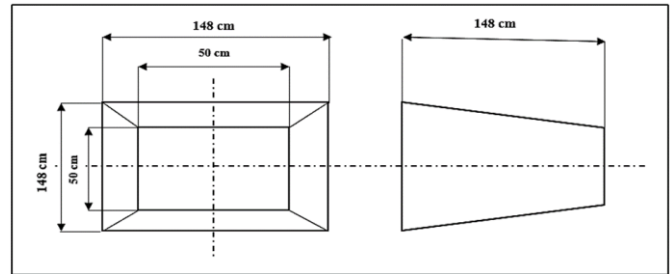


Figure 2. Schematic bell mouth

2.2 Bell mouth

The second part is straight duct, as shown in Figure 3, and involves five sections of equal length; each part is 1 m long and has a 50 cm square side cross-section, as demonstrated in schematic Figure 4. The first section contains an electrical heater to raise the air temperature in order to ($T_{in}=43^{\circ}\text{C}$) enhance the water droplet evaporation such that the required humidity in the air can be achieved. The second part contains a matrix nozzle; this is to ensure that full development occurs to increase the surface contact area between water droplets and the airstream, reduce the air temperature, and therefore enhance the evaporation cooling process. The thermocouple was placed in all five sections evenly to see how much the air temperature dropped along the test tube. The test section is attached to the bell mouth upstream and downstream, joining the axial fan. The mean velocity in the straight duct was selected to be (3, 4, 5, and 7 m/s, respectively).

The parts of the laboratory device were connected by placing an elastic band at the end of each clip to ensure that air did not leak and then fastening with screws.



Figure 3. Test section

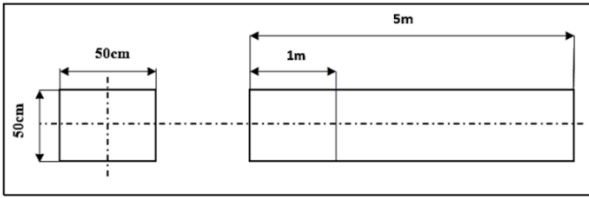


Figure 4. Schematic straight duct

2.3 Axial fan

The last section has the following dimensions: 107 cm long, 50 cm at the inlet square cross section, and 70 cm at the outlet section. The fan is driven by an electric motor of capacity 850 W, type VIE-60Z4B, with a flow rate of 11000 m³/h, a blade diameter of 60 cm, and an air speed of 7.7 m/s, as demonstrated in Figure 5.



Figure 5. Axial fan

3. HUMIDIFICATION SYSTEM

The objective of the humidification system is to provide the humidification needed by introducing pressurized water into the air stream through a straight duct, such that it cools down as well as increases the humidity of the air. It consists of a water tank, pipes, a water pump, valves, and fog nozzles.

3.1 Water tank

To prevent any heat from the surrounding environment from interfering with the cooling process, the outer surface of a galvanized steel box with a 30-cm-sided cube was insulated with rubber foam insulation material with a thermal conductivity of 0.036 W/mK to maintain the water temperature at no more than 22°C. The tank was used to store 25 liters of water, utilized in the humidification process and compensate for the continuous feeding of water during the system's operation. The required amount of water is maintained through the water filter system located in the laboratory.

3.2 Water pump

To generate a high-pressure pump to ensure small streams of water through the nozzles inside the wind tunnel, rubber pipes were used as connections between the water tank and the pump nooses. Figure 6 showed the water pump.

3.3 Fog nozzles

To produce microdroplet size, increase the heat transfer

through surface contact area between water droplets and the airstream, and enhance the evaporation cooling process, Figure 7 presents the dimensions. In this study, the number of nozzles is 9, with a diameter of 0.3 mm. The atomizer was located at (1.7) m. When FD occurs from the beginning of the first duct, the atomizer's horizontal location is parallel to the air flow, as illustrated in Figure 8, which gives better evaporative cooling of air from both experimental work and numerical simulation. The atomizer's horizontal location is parallel to the airflow. Both of these variables have an influence on the droplet's ejecting velocity and size. On the experimental investigation side, a water bubble with a diameter of 100 microns was taken according to the specifications of the nozzle. The amount of water flow required for each hostel is estimated at 85 ml/l.

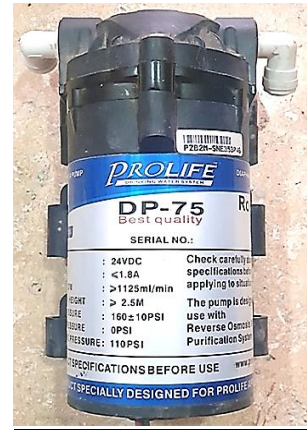


Figure 6. Water pump

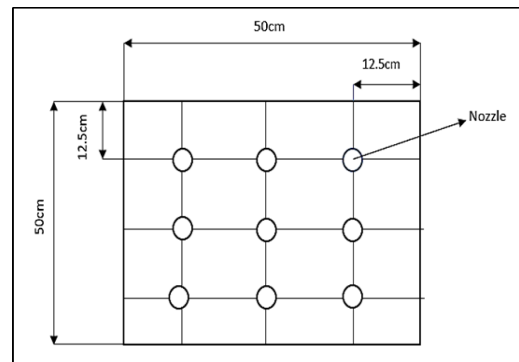


Figure 7. Schematic nozzle inside test rig



Figure 8. Nozzle matrix

3.4 Control electrical heater

In order to increase the air temperature entering the test tunnel to 43°C to improve the process of evaporation of volatile water droplets and increase humidity. The heater used is of capacity (9 kW), and the outer surface is a finned tube, as shown in Figure 9. A heat control system was used to control the heat of the electrical heater with a voltage regulator with a capacity of 100 A, as shown in Figure 10. When the air passes through the heater, it is heated, then it passes to the thermostat, which senses the air temperature, so if it is 43°C, then the control system cuts off the heaters.



Figure 9. Finned electrical heater

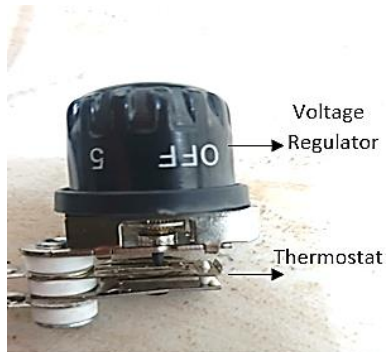


Figure 10. Voltage regulator

4. THEORETICAL ANALYSIS

The thermal performance of the fogging cooling process using a water spray system injected into the main airflow was evaluated. Moreover, numerical analysis of a straight duct with different numbers of nozzles shows the effect on the air temperature. A number of heat equations were used to find and

analyze the results.

4.1 Reynold's number

To find out the type of flow is expressed as [12]:

$$Re_a = \frac{U D_h}{\nu} \quad (1)$$

where,

U: The air velocity in the duct, (m/sec).

D_h: The hydraulic diameter (m).

ν: The kinematic viscosity of the air (m²/ sec).

The duct hydraulic diameter [13]:

$$D_h = \frac{4A}{P_d}$$

where,

(A) is the cross-sectional area,

(P_d): the perimeter of the duct.

4.2 Heat transfer rate

To find the heat transfer rate of the air inner duct [14].

$$Q_{air} = \dot{m} C_p (T_i - T_o) \quad (2)$$

where,

\dot{m} air is the mass flow rate of the air (kg/sec).

C_p is the specific heat of the air (J/kg.K).

T_i is the air outlet temperature (°C).

T_o is the air inlet temperature (°C).

4.3 The cooling effectiveness

The efficacy idea can be used to assess any heat transfer technique. The efficacy effectively contrasts the temperature reduction that can be achieved with the one that may be used, which is the process potential. Effectiveness is provided by:

$$\varepsilon = \frac{t_{db,i} - t_{db,o}}{t_{db,i} - t_{wb,i}} \quad (3)$$

where,

ε = direct evaporative cooling or saturation effectiveness, %.

t_{db,i} = dry-bulb temperature of entering air, °C.

t_{db,o} = Average dry-bulb temperature of leaving air, °C.

t_{wb,i} = wet-bulb temperature of entering air, °C.

4.4 Cooling range

The cooling range is basically the difference between the inlet and outlet temperatures of the free air stream involved in the humidification process. The better the cooling process, the larger the cooling range, which is defined by:

$$\text{Cooling rand} = T_{db,i} - T_{db,o} \quad (4)$$

where,

T_{db,j} = Inlet dry bulb temperatures.

T_{wb,o} = Out dry bulb temperatures.

4.5 The model assumptions and boundary conditions

The cooling range is basically the difference between the

inlet and outlet temperatures of the free air stream involved in the humidification process. The better the cooling process, the larger the cooling range, which is defined by:

A number of assumptions were developed before the numerical analysis was carried out:

- 1- Steady turbulent flow.
- 2- Single-phase fluid in the wind tunnel.
- 3- Maintain a constant inlet temperature.
- 4- The heat exchanger does not generate heat.
- 5- Radiation heat transfer is not considered.
- 6- Adiabatic of the wall wind tunnel.

The boundary condition is clear in Figure 11. To simulate a numerical investigation, the inlet air temperature was 43°C with an air velocity of 3, 4, 5, and 7 m/sec.

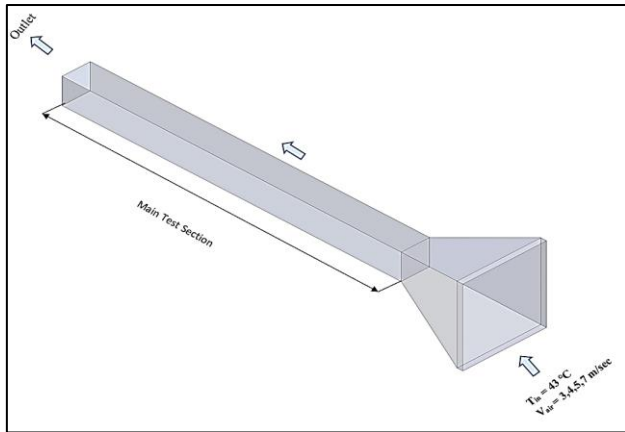


Figure 11. The boundary conditions of the test rig

4.6 Convergence criteria

The iterations stopped when the numerical solution met the selected convergence criteria. In this numerical analysis, 512 iterations were used, and after that, 220 iteration turns were required to finish under suitable values. Figure 12 illustrates the correspondence between numerical and experimental analysis was confirmed by the validation.

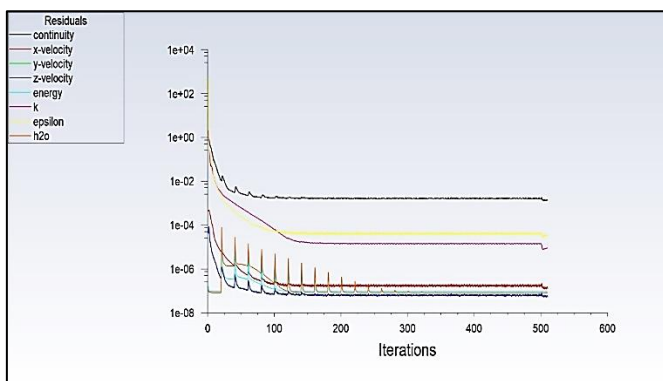


Figure 12. The Convergence of numerical simulation

5. RESULTS AND DISCUSSION

Experimentally, several models of spray were injected into the flow of air at different numbers of nozzles and velocities. In order to analyze and study the results extracted from the numerical side to evaluate the performance enhancement of the system.

5.1 Validation of the numerical transient simulation

In the current study, a numerical simulation has been carried out and validated against experimental results. Find out how close the results and behavior are between experimental and numerical. Figures 13 and 14 exhibit the predicted measured temperature distribution as a function of axial distance with a velocity of 3 m/s. In addition, the number of nozzles was 5 and 9, respectively, and the wind tunnel was divided into 5 portions after the nozzle matrix to study the temperature variation. The results manifested that an acceptable agreement has been acquired with a maximum error of 1.1% and 2.5%, respectively, for temperature drops. Figure 14 shows the numerical prediction.

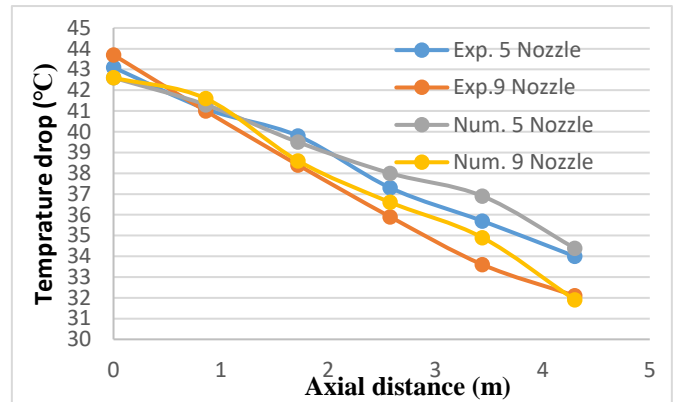
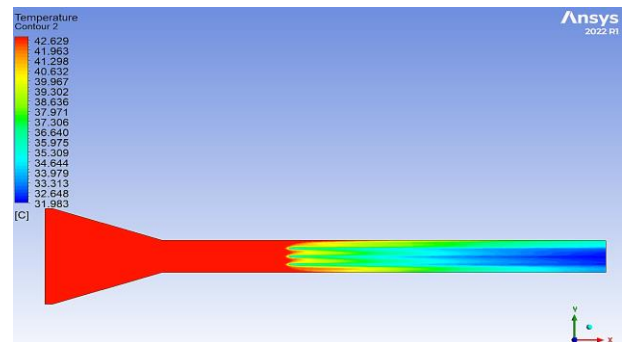
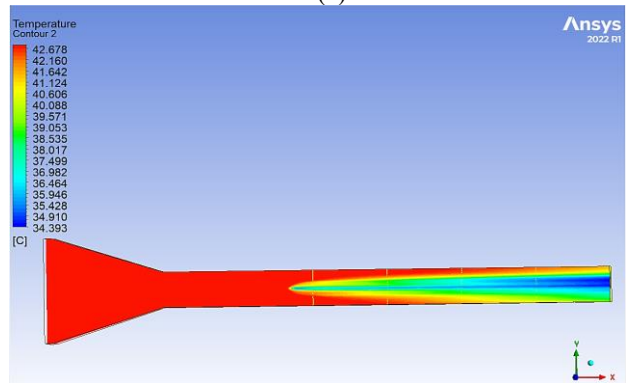


Figure 13. The numerical validation of temperature drop



(a)



(b)

Figure 14. Temperature contour velocity (a) 9 nozzle (b) 5 nozzle

5.2 Heat transfer rate

The heat transfer rate dropped along the axial distance, as presented in Figure 15. This reduction in heat transfer rate

occurs when heat is transferred forward. In the beginning, because of the entry of dry air, heat exchange occurs between the droplet and the hot air, which is high. This improvement in the heat exchange process cools the hot air entering the compressor and thus increases the power output after the temperatures converge due to equal temperatures. The amount of heat improvement was 29.3% and 37.7%, respectively.

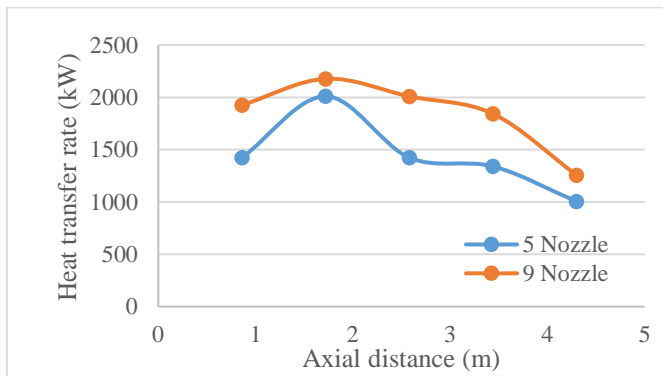


Figure 15. Illustrated heat transfer

5.3 Thermal efficiency

Figure 16 expresses the thermal efficiency of the experimental results in Baghdad, Iraq. It could be noted that the average deviation of experimental results is about 10.4%, while it reached 10% in comparison with conditions similar to our working conditions [15]. The reduction in thermal with increased ambient temperature in the selected months is caused by the reduction in mass flow reduction, which is also a result of the reduction in density of air, and air entering the compressor is dry, which reduces combustion quality. As the inlet air temperature increases in the hot months, the power output decreases.

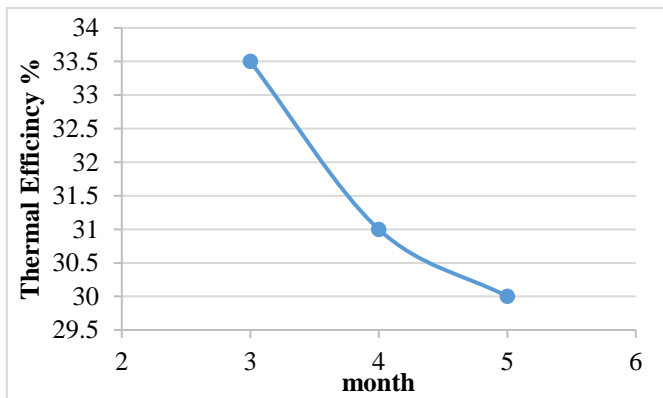


Figure 16. Illustrated thermal efficiency

5.4 Thermal efficiency

The efficacy idea, as shown in the equation, can be used to assess any heat transfer technique (3). The efficacy effectively contrasts the temperature reduction that can be achieved with that which may be used, which is the process potential. One of the most helpful pieces of information is the temperature drop attained.

Due to a longer time period for the heat exchange between water droplets and the airstream, the velocity (3 m/s) depicted

in Figure 17 provides the most substantial improvement in the evaporative cooling process compared to other velocities. Under these circumstances, at a velocity of 3 to 7 m/s with 9 and 5 nozzles, the highest effectiveness was 43%, followed by 30.7%, respectively. This improvement increases the output of electrical energy, and as the cooled air has a high density, this improves the combustion process unlike dry air.

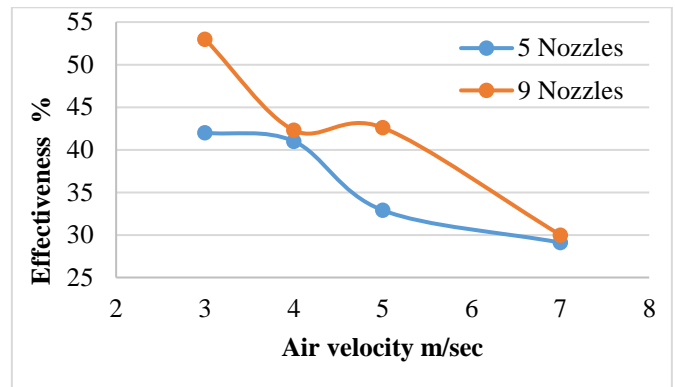


Figure 17. Variation of cooling effectiveness with induced air flow rate

5.5 Ambient temperature

According to Figure 18, the increase in ambient temperature will improve the humidification of the air as well as the range of cooling that is attainable. This effect is attributable to the fact that hot air is usually less humid and can absorb more water vapor. The reduction in the air temperature for a 43°C inlet temperature was 25.3%, whereas for the normal ambient temperature of 36.8°C, the reduction was no more than 19% at a velocity of 3 m/s and 9 nozzles.

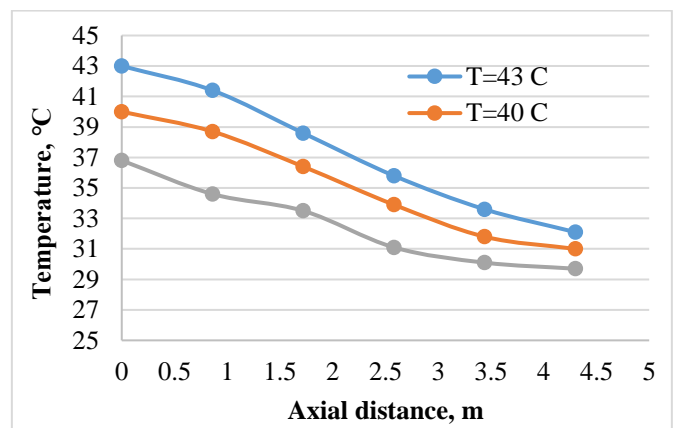


Figure 18. Effect of ambient air temperature of air temperature

5.6 Cooling range

Figure 19 explains the result of increasing the ambient air temperature in the cooling range. The increase in ambient air temperature leads to better humidification as well as a drop in temperature due to the less humid stream's higher ability to contain water vapor. That increasing the temperature from 36.8 to 43°C leads to an increase in the drop temperature range from 7.1 to 10.9°C.

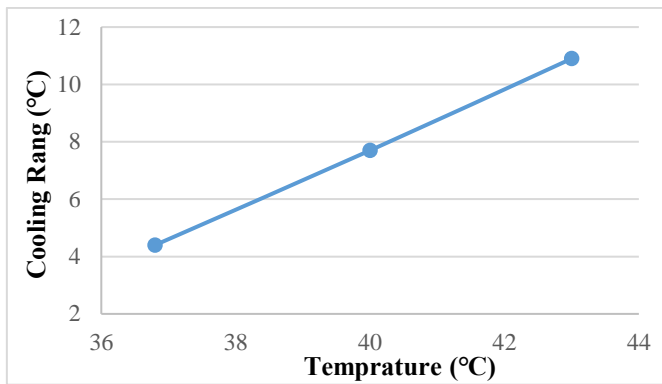


Figure 19. Variation of cooling range with ambient air temperature

6. CONCLUSIONS

The most important results obtained throughout this study were obtained experimentally in order to evaluate the performance of the fogging system installed at the inlet of the wind tunnel.

1. The results manifested that an acceptable agreement has been acquired with a maximum error of 2.5% for temperature drop.

2. The heat transfer can be enhanced with nine nozzles to reach 37.7%.

3. Thermal efficiency deteriorates with increasing ambient temperatures in the month by about 10.4%.

4. Effectiveness begins with improvement at low velocities and then deteriorates due to increasing air velocities and not allowing enough time for heat exchange.

5. The high temperature dropped to 25.3%, better than the normal ambient temperature.

6. With an increase in the ambient air temperature, the cooling range will improve.

7. Improve the operation cost to 28.5% when using nine nozzles.

Recommendations for future work based on the present work: The following recommendations Future research will increase the number of nozzles by changing the hole of the nozzle. Develop the number of air entry openings with a gate to control airflow. Find the energy analysis and cost-benefit ratio.

ACKNOWLEDGMENT

The authors would like to thank Mustansiriyah University (www.uomustansiryah.edu.iq) Baghdad-Iraq for its support in the present work.

REFERENCES

[1] Egware, H.O., Onochie, U.P., Itoje, H. (2020). Effect of incorporating fogging inlet air cooling system: A case study of Ihovbor Thermal Power Plant, Benin City. *International Journal of Ambient Energy*, 43(1): 2173-2179. <https://doi.org/10.1080/01430750.2020.1722231>

[2] Deng, C., Al-Sammarrai, A.T., Ibrahim, T.K., Kosari, E., Basrawi, F., Ismail, F.B., Abdalla, A.N. (2020). Air cooling techniques and corresponding impacts on

combined cycle power plant (CCPP) performance. *International Journal of Refrigeration*, 120: 161-177. <https://doi.org/10.1016/j.ijrefrig.2020.08.008>

[3] Ikpe, A.E., Iluobe, I.C., Desmond Imonitie, I. (2020). Modelling and simulation of high pressure fogging air intake cooling unit of Omotosho phase II gas turbine power plant. *Journal of Applied Research on Industrial Engineering*, 7(2): 121-136. <https://doi.org/10.22105/jarjie.2020.216680.1129>

[4] El-Zahaby, A.M., El-Samadony, Y.A.F., El-Fakharany, M.K., Gheath, A.A. (2017). Enhancing gas turbine plant performance in hot climates through fogging technique. *International Journal of Scientific & Engineering Research*, 8(6): 1845-1848.

[5] AL-Jibory, M.W., Rashid, F.L., Hussein, H.Q. (2020). Review of heat transfer enhancement in aircooled turbine blades. *International Journal of Scientific & Technology Research*, 9(4): 3123-3130.

[6] Radchenko, A., Trushliakov, E., Kosowski, K., Mikielewicz, D., Radchenko, M. (2020). Innovative turbine intake air cooling systems and their rational designing. *Energies*, 13(23): 6201. <https://doi.org/10.3390/en13236201>

[7] Hasan, M.J., Tawkir, K., Bhuiyan, A.A. (2022). Improvement of an exhaust gas recirculation cooler using discrete ribbed and perforated louvered strip vortex generator. *International Journal of Thermofluids*, 13: 100132. <https://doi.org/10.1016/j.ijft.2022.100132>

[8] Yu, Z., Cao, Q., Liu, Z., Liu, B. (2021). Study of impingement cooling technology by using circular pin fins and mist/air methods in gas turbine combustor. *Journal of Physics: Conference Series*, 2235: 012092. <https://doi.org/10.1088/1742-6596/2235/1/012092>

[9] Kore, S.S., Dingare, S.V., Chinchankar, S., Hujare, P., Mache, A. (2020). Experimental Analysis of different shaped ribs on heat transfer and fluid flow characteristics. *Web of Conferences*, 170: 01019. <https://doi.org/10.1051/e3sconf/202017001019>

[10] Gulave, J.S., Desale, P.S. (2015). Review of heat transfer enhancement techniques of W Ribs. *International Journal of Scientific Engineering and Research*, 5(5): 175-178. <https://www.ijser.in/archives/v5i5/IJSER151503.pdf>

[11] Dinc, A., Elbadawy, I., Fayed, M., Taher, R., Derakhshandeh, J.F., Gharbia, Y. (2021). Performance improvement of a 43 MW class gas turbine engine with inlet air cooling. *International Journal of Emerging Trends in Engineering Research*, 9(5): 539-544. <https://www.warse.org/IJETER/static/pdf/file/ijeter01952021.pdf>

[12] Tawackolian, K., Kriegel, M. (2022). Turbulence model performance for ventilation components pressure losses. *Building Simulation*, 15(3): 389-399. <https://doi.org/10.1007/s12273-021-0803-x>

[13] Weisz, T.G., Müller, B., Kristoffersen, R. (2023). Simulation of flow in the human upper airways modeled as a piping system using the hydraulic diameter. In *Proceedings of the 63rd International Conference of Scandinavian Simulation Society, SIMS 2022, Trondheim, Norway*. <https://doi.org/10.3384/ecp192033>

[14] Alrwashdeh, S.S., Handri, A., Madanat, M.A., Al-Falahat, A.M. (2023). The effect of heat exchanger design on heat transfer rate and temperature distribution. *Emerging Science Journal*, 6(1): 128-137. <https://doi.org/10.28991/ESJ-2022-06-01-010>

[15] Kumaria, N., Bahadur, V., Hodes, M., Salamon, T., Kolodner, P., Lyons, A., Garimella, S.V. (2010). Analysis of evaporating mist flow for enhanced

convective heat transfer. *International Journal of Heat and Mass Transfer*, 53(15-16): 336-3356. <https://doi.org/10.1016/j.ijheatmasstransfer.2010.02.027>